Oxygen adsorbed on oxidized Ru(0001)

Artur Böttcher* and Horst Niehus
Institut für Physik der Humboldt-Universität zu Berlin, Invalidenstrasse 110, 10115 Berlin, Germany
(Received 24 November 1998; revised manuscript received 22 February 1999)

An atomic oxygen species adsorbed on Ru(0001) containing subsurface oxygen has been found and is characterized by the means of thermal description spectroscopy (TDS), ultraviolet photoemission spectroscopy, and reactive CO scattering. The surplus oxygen can be adsorbed on an oxygen-rich ruthenium crystal at room temperature when more than two monolayers of oxygen are deposited in the subsurface region (1 ML $=1.58\times10^{15}$ cm^{-2}). The maximum number of oxygen atoms occupying this state depends on the oxygen content in the subsurface region. It saturates for oxygen contents higher than about 10 ML at a level of 0.25 ML. The initial binding energy of an adsorbed oxygen atom, as derived from TDS data, is lower than 0.75 eV per atom. It continuously decreases with increasing lateral adatom density. The work function ϕ varies with the increasing population of this oxygen state. For saturating oxygen coverage it reaches a maximum that can be by 1.3 eV higher than the value known for a clean metallic Ru surface. The CO oxidation was performed in a beam scattering experiment and it reveals a high reactivity of this weakly bound state. At room temperature the CO/CO_2-conversion probability reaches a value of 0.18, which is nearly by one order of magnitude higher than the one found for subsurface oxygen at much higher temperatures. [S0163-1829(99)12243-4]

I. INTRODUCTION

Interaction of oxygen molecules with transition metal surfaces proceeds in most of the cases via dissociative chemisorption.[1–3] This reaction stage usually results in the formation of a saturated adsorbed oxygen layer. Such a lateral saturation has been investigated under ultra high vacuum conditions (UHV) at the Ru(0001) surface.[4–6] It manifests itself in a pronounced increase of the surface work function as well as by a reduced binding energy of the adatoms.[4] The substantially weakened O-Ru bond is very attractive to surface processes where atomic oxygen is involved. It promises a large enhancement of the reaction yield.[5,7] The chemisorption does not stop with the saturation of an adsorbed phase. Further exposure leads to oxygen penetration into the subsurface region of the sample.[8–12] This process proceeds with a rather low probability per impinging oxygen molecule. It does not overcome a limit of 10^{-6} for samples kept at room temperature. However, it can easily be increased by raising the surface temperature.[8] Despite the low probability, the dissolution of oxygen obviously becomes a very efficient surface-mediated process when performed at higher partial pressure. The resulting subsurface-oxygen phase exhibits some new interesting properties.[8–12] Despite the high-oxygen content, the surface does not lose its original metallicity, it behaves like a reservoir of mobile atomic oxygen. The oxygen dissolution is limited and gradually replaced by the formation of regular oxides (RuO_4,RuO_2) when continuing the exposure at sample temperature higher than about 750 K.[8,14] The oxides created this way terminate a series of numerous oxygen species appearing in the course of oxygen chemisorption.

Recently, it has been convincingly demonstrated that the CO oxidation performed at an oxygen-rich Ru(0001) surface, becomes more efficient by two orders of magnitude when the sample has contained subsurface oxygen.[13] Such a pronounced reactivity jump obviously motivates more detailed investigations of the subsurface-oxygen phase.

We report here on an oxygen species, which appears on the topmost layer of a surface only, when the crystal contains a considerable amount of oxygen dissolved in the subsurface region. This new phase exhibits quite distinct electronic and chemical properties, which allow to distinguish it easily from the remaining three oxygen species mentioned above.

In the first section, we present some experiments that show the presence of an oxygen phase and simultaneously determine all relevant conditions for its formation. In the second part, by combining thermal desorption spectroscopy (TDS) and ultraviolet photoemission spectroscopy (UPS) experiments, some thermodynamic and electronic properties of the adsorbed oxygen species become evident. Finally, with the example of CO/CO_2-conversion, as it takes place over an oxygen-rich surface, the reactivity of this new oxygen state will be characterized. The short characterization will be completed by discussing the relevance of this topmost oxygen species for high-pressure CO oxidation.

II. EXPERIMENTS

The experiments were performed in an ultrahigh vacuum (UHV) apparatus with a base pressure better than 10^{-10} mbar. The main analytical chamber is equipped with low-energy electron diffraction (LEED) optics (Varian) a quadruple mass spectrometer (Extranuclear), an ultraviolet photoelectron spectrometer, UPS (Omicron) and a sputtering Ar^+-gun. This chamber is connected to a two stages supersonic molecular beam apparatus that has been designed to perform reactive scattering measurements as well as thermal energy atomic scattering.[15] The molecular beam is mechanically chopped with a constant frequency in the range of 70–500 Hz and the scattered molecules can be detected by the means of a specularly arranged mass spectrometer ($\phi_{in}=\phi_{out}$) with a phase-sensitive lock-in mode, or by monitoring the partial pressure. The molecular beam is formed by a

supersonic gas expansion through a nozzle which can work at 900 K for many hours without a significant increase of the background-pressure. High-molecular flux in the range of $3-6\times10^{14}$ molecules/cm^{2}s can be achieved without perturbing the beam quality (velocity distribution, divergence, etc.). The beam spot is centered at the ruthenium surface and covers 80% of the whole sample area of 0.5 cm^2.

The Ru crystal was mounted using tungsten wires in two slits on the sample edges. The wires are used as resistive heaters and simultaneously as heat exchangers. An efficient nitrogen cooling system prevents an unwanted heat expansion from the strongly heated sample to the metallic holders and consequently the background pressure does not exceed a range of 2×10^{-10} mbar even when keeping the sample at 1100 K for some minutes. The sample temperature was measured by a Ni-Cr/Ni-thermocouple spot welded to the back side of the sample. The Ru(0001) surface was cleaned by a standard cleaning procedure described by Madey *et al.*[2] The sample was treated by a series of sputtering and oxidizing cycles followed by some annealing flashes up to 1550 K. The resulting degree of roughness was macroscopically characterized by specular He scattering.[15] The chemical cleanliness was verified by ultraviolet photoelectron spectroscopy (UPS) and thermal desorption spectroscopy (TDS).

The subsurface oxygen phase was created by exposing the sample to a partial oxygen pressure of 10^{-3}–10^{-2} mbar at a constant surface temperature in the range of 400–750 K. The resulting oxygen content has been determined by monitoring the recombinatively desorbed molecular oxygen and by integrating the resulting TD spectra. In this work the oxygen contents are given in monolayers, i.e., relative in the number of substrate surface atoms. An oxygen coverage corresponding to the monolayer, $\Theta_0=1$, has been found by relating the appearance of the 1×1 LEED pattern to the O_2-TD spectra. The lateral density of oxygen atoms corresponding to the saturated monolayer reaches a value of 1.58×10^{15}cm^{-2}. All coverages are expressed in terms of a monolayer (ML). All TD spectra were taken at a constant heating rate of 6 K/s.

III. RESULTS AND DISCUSSION

A. Formation of an adsorbed state

Figure 1 shows a typical O_2 thermal desorption spectrum (TDS) recorded after an exposure of the Ru(0001) surface to 1.5×10^6 L oxygen at 750 K. Three distinct features can easily be seen on this spectra. The broad high-temperature region ($A, T>1100$ K) originates from the associative desorption of atomic oxygen adsorbed on a clean metallic surface.[2,3] The chemisorptive interaction of a single oxygen atom with the ruthenium surface belongs to the strongest bonds and is characterized by a binding energy of 3.5 eV.[2] At higher oxygen coverages, the lateral O-O interaction reduces this energy to 1.8 eV.[7,8] In this situation a two-dimensional adsorbed layer becomes completed and it finally forms the 1×1-O superstructure as revealed by LEED and density-functional theory (DFT) studies.[4,5] The most intense desorption feature (*B*) represents the desorption of oxygen that has been deposited in the subsurface region.[8–10] The desorption profile results from a recombination of topmost oxygen atoms with the subsurface oxygen, O_{sub}, atoms which finally escape as oxygen molecules, and the desorption kinetics is determined by oxygen diffusion from the subsurface region towards the surface.[8,9]

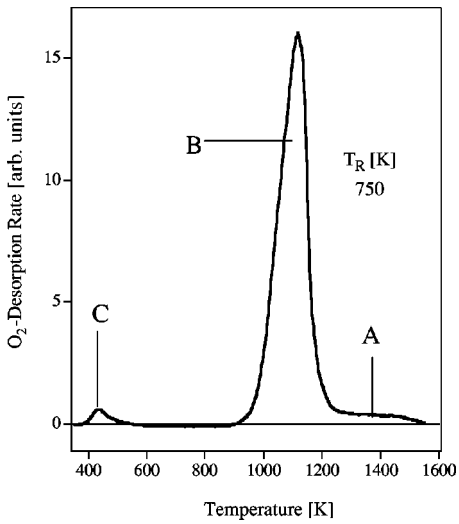

FIG. 1. O_2 thermal desorption spectrum recorded from the Ru(0001) surface exposed to 1.5×10^6 L of oxygen at a fixed sample temperature of 750 K. While the sample was cooling down to room temperature, the partial oxygen pressure slowly reached a value lower than 1×10^{-10} mbar. The state labeled by *A* represents the oxygen desorption from a 2D layer adsorbed on a clean metallic Ru surface. The most intense feature *B* has been attributed to the desorption of the subsurface oxygen. The weak TD peak labeled by *C* represents atomic oxygen adsorbed on oxide domains.

In a temperature region between 300 and 550 K an additional, less intense, oxygen desorption feature (*C*) appears. The presence of this peak at a rather low-temperature range is somewhat surprising, because the crystal has been exposed to oxygen at a much higher temperature than 550 K. However, the preparation procedure is not completed by closing the valve and turning off the sample heater. The post-heating exposure stage in which the sample temperature decreases from 700 K to room temperature and the partial oxygen pressure slowly reaches the base pressure (10^{-10} mbar), usually takes a few minutes. Within this period further oxygen adsorption is not excluded and state *C* can gradually be formed. When the sample is kept at 700 K after stopping the oxygen dosage until the pressure in the chamber reaches the base value, peak *C* is completely absent. To avoid misunderstandings, we will in the following passages use the terms, adsorbed phase, or adsorbed oxygen atoms, only for oxygen deposited on an oxygen-rich Ru surface where state *C* can be created.

In order to guarantee that the prepared surface containing the subsurface oxygen is not covered by any adsorbed oxygen, $\Theta_{ad}=0$, the sample has been flashed to 600 K only when the pressure in the chamber was lower than 10^{-10} mbar. Subsequently, the adsorption state was formed by exposing such a surface at room temperature to a certain oxygen dose. The resulting occupation of this state was measured by integrating the corresponding oxygen desorption spectrum.

It has to be noted, that the desorption peak *C* represents a well defined separate oxygen phase without any admixture from the remaining phases *A* or *B*. In the temperature range of 300–600 K, no oxygen desorption could be observed

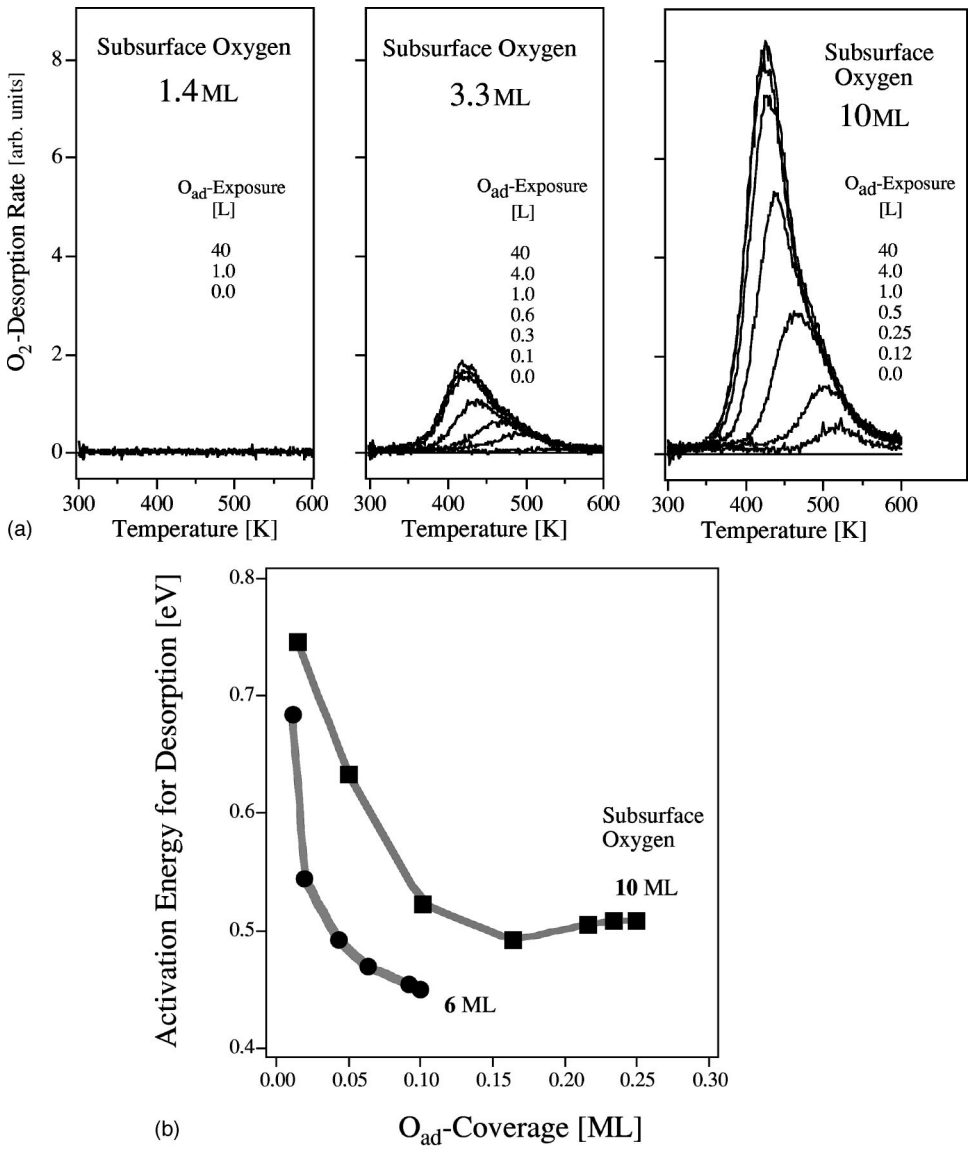

FIG. 2. (a) Three oxygen-rich Ru surfaces containing different amounts of oxygen (1.4, 3.3, and 10 ML, from left to right panel, respectively) were subsequently exposed to a variety of oxygen doses at a fixed sample temperature of 300 K, and the Fig. 2(a) shows the corresponding O_2 TD spectra recorded afterwards. All TD spectra were monitored at a constant heating rate of 6 K/s. (b) The activation energy for oxygen desorption is shown as a function of an increasing occupation of the adsorbed state *C* created at surfaces containing 6 and 10 ML of subsurface oxygen, circles and squares, respectively. The values were derived assuming the second-order desorption kinetics.

without performing a exposure of the sample to oxygen. This adsorption-desorption cycle was repeated many times without measuring significant changes in the recorded desorption profiles. Such a behavior indicates a rather high-thermal stability of the surface sites responsible for the binding of oxygen.

Now, we will look for physical conditions for formation of the adsorbed oxygen state. First, we checked how the population of state *C* depends on the oxygen content in the subsurface region. Figure 2(a) shows O_2-TD spectra obtained after depositing small amounts of oxygen onto samples kept at room temperature and differing by the oxygen contents in the bulk: 1.4, 3.3, and 10 ML. Oxygen adsorption onto a ruthenium surface covered only by a saturated oxygen layer (1 ML) does not lead to any desorption features within range *C*. We found the same negative result for slightly higher oxygen contents up to 2.2 ML. The corresponding LEED images exhibited intense spots with the 1×1 symmetry revealing that the surface is terminated by the 1×1-O phase only. For oxygen contents higher than about 3 ML already recognizable desorption profiles *C* were observed [see Fig. 2(a), central panel]. The desorption features become very intense when the sample accommodates large amounts of oxygen (right panel). In such cases the desorption profiles are shaped in a way suggesting a second-order desorption kinetics with a nearly constant preexponential factor.[16] Such profiles are characterized mainly by a pronounced shift of the desorption maximum towards lower sample temperatures with increasing density of adsorbed atoms. We have applied the method proposed by Chan, Aris, and Weinberg[17] for the determination of the activation energy of desorption E_{des}, as a function of the oxygen coverage, Θ_{ad}. Figure 2(b) shows this function $E_{des}(\Theta_{ad})$ obtained for two oxygen contents in the subsurface region, 6 and 10 ML. The initial activation energy for oxygen desorption, $E_{des}(\Theta_{ad}=0)$ ranges from 0.75 to 0.63 eV with decreasing content of subsurface oxygen. For all investigated contents of subsurface oxygen the activation energy, E_{des}, decreases nearly exponentially with the increasing density of the Θ_{ad} phase. The magnitude of this decrease varies from 0.26 eV for a high content of O_{sub} to 0.2 eV for O_{sub} <4 ML. Such an analysis can obviously be applied only for 2D systems in which the lateral pair-wise repulsive O_{ad}-O_{ad} interaction is responsible for the observed lowering of the binding energy. The maximum population of the adsorbed

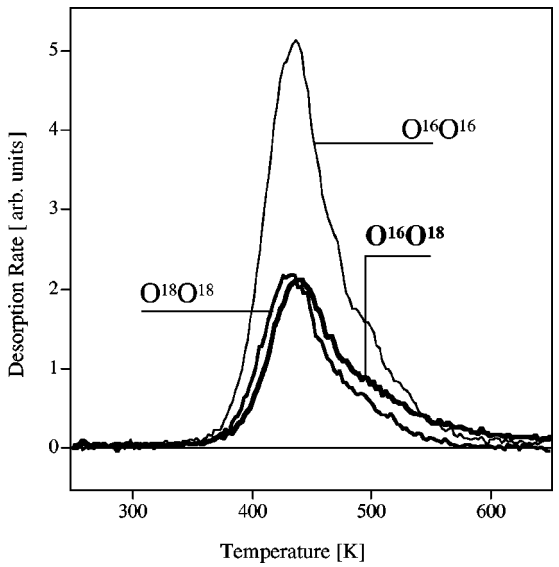

FIG. 3. $^{36}O_2$ and $^{34}O_2$ thermal desorption spectra taken after exposing an oxygen-rich surface (9 ML of $^{32}O_2$) to 100 L of $^{36}O_2$. For comparison the $^{32}O_2$ TD obtained after performing the same procedure by using only $^{32}O_2$.

phase, $O_{ad,sat}$, as found here, is much lower than the coverage corresponding to a monolayer. Consequently we can rather tentatively conclude that these minority oxygen species are arranged in a 2D network.

As shown in Fig. 2(b), in comparison to other known oxygen species the phase stands out because of a rather low-desorption energy (<0.8 eV) which allows us to classify it as a weak chemisorptive bond. It cannot be considered as a case of a strong physisorption, because its binding energy is almost two times higher than the strongest known physisorptive bond (e.g., the Xe/W).[18] It can be, however, compared to the chemisorptive bond of CO molecules on transition metals[19] as well as to the binding of small molecules on surfaces of solid oxides (e.g., NO molecules on a NiO surface).[18] Such bonds are characterized by desorption energies in the range of 0.5–0.6 eV.[18]

Recent DFT calculations performed by Stampfl and Scheffler[7] show an energy gain of 1.2 eV with adsorption of an oxygen atom into an unoccupied site in the 1×1-O/Ru structure. Here of course, this finding cannot be used as a proper concept for the adsorption of surplus oxygen on O_{sub}/Ru because of the additional presence of subsurface oxygen just below the topmost Ru layer. But it might serve as an energetic hint also for the O_{ad} atoms.

As mentioned above the O_2 TD profiles reveal the second-order desorption kinetics. This fact suggests that the new state contains oxygen atoms exclusively. We performed an isotope exchange experiment which supports this hint. The Ru(0001) surface containing about 9 ML of ^{16}O in the subsurface region has been exposed to 100L of $^{36}O_2$ at room temperature. Both masses, $^{34}O_2$ and $^{36}O_2$ were monitored simultaneously by a mass spectrometer during a subsequent thermal desorption scan. Figure 3 shows the $^{36}O_2$ and $^{34}O_2$ TD traces in comparison with the desorption profile taken when the state was occupied by $^{32}O_2$ only. The main message of this result is clear, the $^{34}O_2$ signal (mixed from ^{16}O and ^{18}O) proves that state *C* is occupied by oxygen atoms

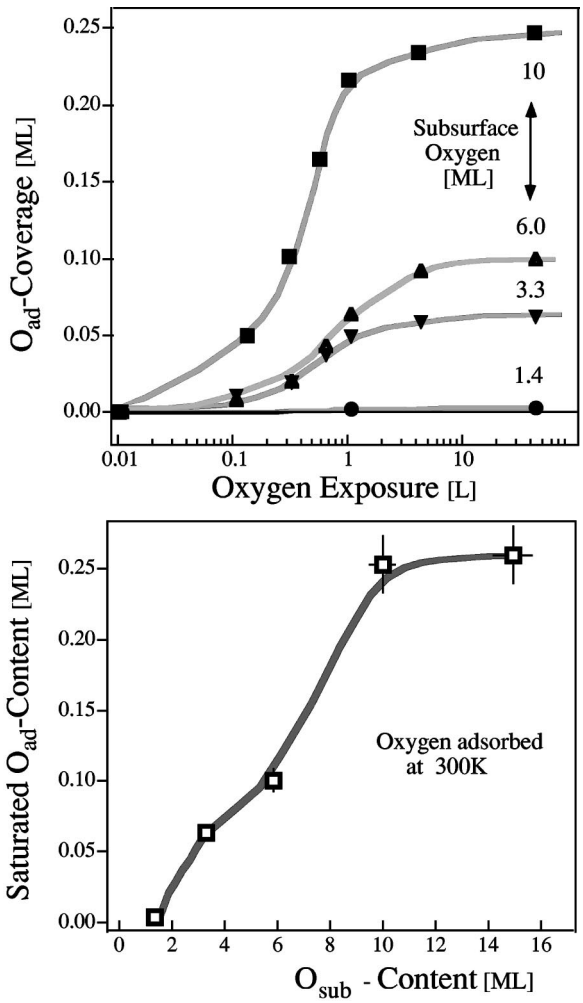

FIG. 4. The upper panel shows the occupation of state *C* versus oxygen exposure, obtained for four samples differing by oxygen contents in the subsurface region (as indicated at the plot). The lower panel shows the maximum occupation of state *C* as a function of the oxygen content in the subsurface region. The deposition of the surplus oxygen was performed at a sample temperature of 300 K.

resulting from the dissociation of impinging molecules. The probing ^{18}O atoms can recombine with the same atomic isotopes as well as with previously deposited ^{16}O atoms that form the adjacent environment of the state.

The fact, that the oxygen-rich Ru surface conserves its initial ability to dissociate the impinging oxygen molecules surprises somewhat. However, it becomes intelligible when considering that the 1×1-O oxygen phase is not the only constituent of the topmost surface layer. Possible defect structures in the oxygen layer might be formed via a local transformation of the subsurface-oxygen into oxides. Indeed, the LEED pattern obtained for samples for which state *C* can be occupied show both, the substantially weakened 1×1 spots as well as some additional weak and less ordered features, which signalize the formation of a distinct phase. Thus, in contrast to the 1×1-O phase, the surface domains exhibit the ability to dissociate the chemisorbing molecules and to accommodate the atomic dissociation products.

The upper panel in Fig. 4 shows uptake curves for oxygen adsorption onto surfaces containing distinct amounts of sub-

surface oxygen. The current occupation of state *C* has been obtained via integrating the O_2 TD spectra and comparing the values with the ones measured for a completed adsorbed layer, 1×1-O/Ru. It can easily be seen that the adsorbed state becomes completed already at a rather low-oxygen exposure of about 10 L, independently of the subsurface-oxygen content in the sample. The adsorption kinetics, however, strongly depends on the subsurface-oxygen content. Moreover, the maximum number of oxygen atoms, which can be accommodated in this state, $\Theta_{ad,sat}$, simply increases with the progressing content of oxygen in the subsurface region. The lower panel in Fig. 4 shows the maximum population of the adsorbed state, $\Theta_{ad,sat}$, as a function of the subsurface-oxygen content. For low contents it increases nearly linearly, and it saturates at 0.25 ML for O_{sub}-contents higher than about 10 ML. The latter two findings (Fig. 4), i.e., the relation between the $\Theta_{ad,sat}$ and the O_{sub}-content, become clear when considering the preparation procedure applied here to achieve different oxygen contents. Simply, the large oxygen contents were obtained by raising the sample temperature during the oxygen exposure. At elevated temperatures both, the oxygen dissolution as well as the formation of local oxide phases, become effectively activated. Thus, oxide like surface domains coexist with the 1×1-O regions to an extent, which depends on oxidation conditions. In that sense, the $\Theta_{ad,sat}$ as the function of O_{sub}-content mirrors the formation of adsorption sites probably induced by the oxide growth. At the moment the atomic nature of these adsites remains unclear. Presumably some embedded oxide molecules as precursors of a regular oxide phase can offer active sites when theirs Ru-4*d* derived orbitals, still not involved in the bond with adjacent oxygen atoms, act as a kind of oxygen acceptors. This idea corresponds to the binding theory of small molecules on oxygen deficient surfaces of MgO and NiO.[20,21]

By relating the uptake curves (Fig. 4) to the $\Theta_{ad,sat}$, as a simple measure of the available adsites, the time evolution of the sticking coefficient could be reconstructed. A rough estimation of the initial sticking probability for impinging oxygen molecules S_{init}, leads to values higher than about 0.7, which is much higher than the one measured for oxygen chemisorption onto a clean Ru(0001).[22] It has to be mentioned that the probability for dissociative sticking of an oxygen molecule onto a homogeneous 1×1-O phase at room temperature has been found to be lower than 10^{-6}.[8] This intriguing finding stimulated us to undertake an additional measurement of the sticking coefficient according to the King-Wells molecular beam method.[23] Figure 5 shows the time evolution of the sticking coefficient as measured by scattering the oxygen beam on a clean Ru surface (curve a) as well as on a surface containing about 9 ML of oxygen in the subsurface region (curve b). Both experiments were performed at exactly the same conditions (crystal temperature of 300 K, the flux of oxygen molecules of 3×10^{14} $cm^{-2}s^{-1}$, impact angle 22.5°). The value of the initial sticking probability obtained here for clean Ru(0001) surface of about 0.4 well agrees with the one measured by Wheeler *et al.*[22] The comparison with the oxygen-rich surface is evident, the initial probability for an occupation of state *C* is almost two times higher than the sticking probability onto a clean Ru surface. Furthermore, according to the higher capacity of a clean surface, as a 2D array of adsites, it takes much longer time to reach a saturation than in the case of state *C*.

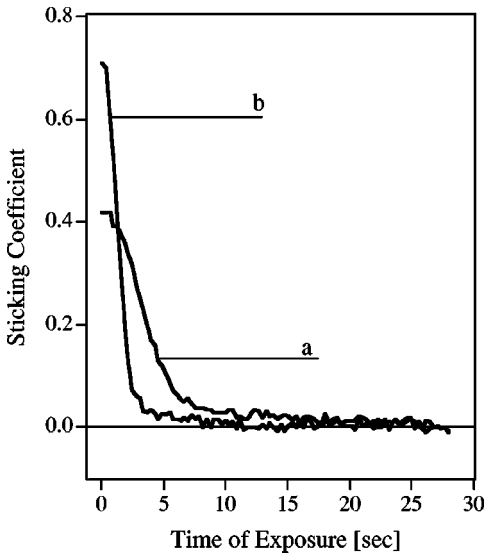

FIG. 5. Time evolution of the sticking coefficient as observed during exposing a clean Ru(0001) surface (curve a) and an oxygen-rich surface (curve b) to the oxygen beam of 3×10^{14} $cm^{-2}s^{-1}$. Both experiments were performed at sample temperature of 300 K.

Summarizing, despite the large oxygen contents already deposited, the oxygen-rich Ru surfaces exhibit an anomalous ability to dissociate and accommodate oxygen even at room temperature. This capacity is represented by state *C*.

B. Electronic properties of the adsorbed state

The next experiment should clarify how the increasing occupation of the adsorbed state affects the electronic properties of the surface. The difficulties on the way to clearly select the spectroscopic features originating exclusively from the surplus adsorbed oxygen, become evident, when considering the low density of the state ($\Theta_{ad}<0.25$) in comparison with the high content of the subsurface oxygen. Despite the rather negative prediction we first apply the ultraviolet photoionization spectroscopy ($h\nu=21.2$ eV) to monitor the valence energy region. This choice is additionally supported by the fact that all features characteristic for the O-2*p* state are located within a range of 15 eV below Fermi level.[24] First, we analyze such samples which contain rich subsurface-oxygen phase without any traces of the adsorbed state *C*. Unfortunately, as can easily be seen in Figs. 6 and 7, no spectral features could be directly attributed to the adsorbed O-2*p* derived state, and consequently we have to focus on the Ru states, which dominate the spectrum and can be used as a sensitive probe of the oxygen presence. Figure 6 shows UP spectra which illustrate how the presence of oxygen atoms modifies the valence density of states of the ruthenium substrate. The spectrum of a clean surface exhibits three very intense peaks at a binding energy of 0.4, 2.6, and 5.4 eV. A convincing assignment of these peaks has been performed by Hofmann and Menzel.[25] All these features represent direct transitions from Ru-4d bands. The enhanced emission near Fermi energy, marked here by α, is attributed to intrinsic surface resonance. The lower and upper *d* bands appear at 2.6 and 5.4 eV, as peaks β and γ, respectively.

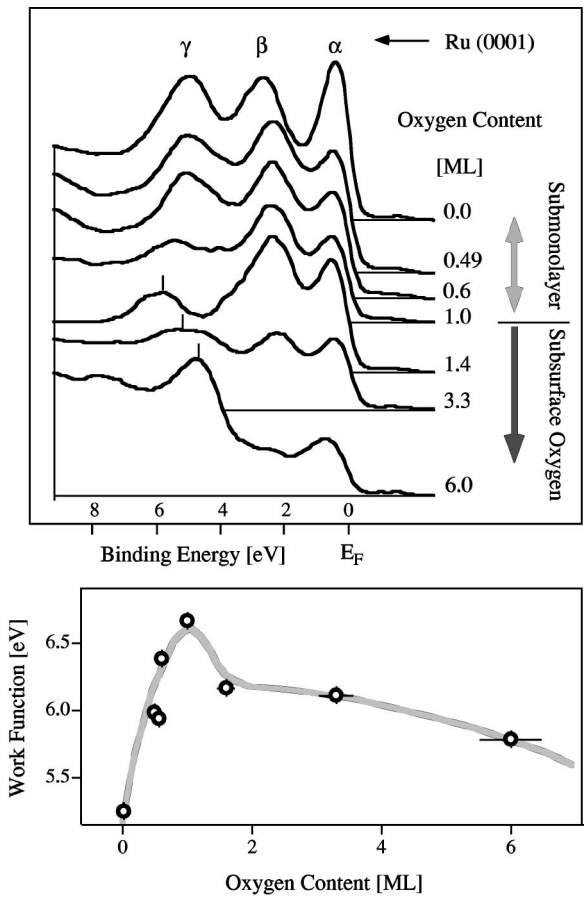

FIG. 6. The evolution of the valence energy region as monitored by means of UP (21.2 eV) spectroscopy during oxygen dissolution into ruthenium crystal (upper frame). The lower frame shows the corresponding changes of the work function.

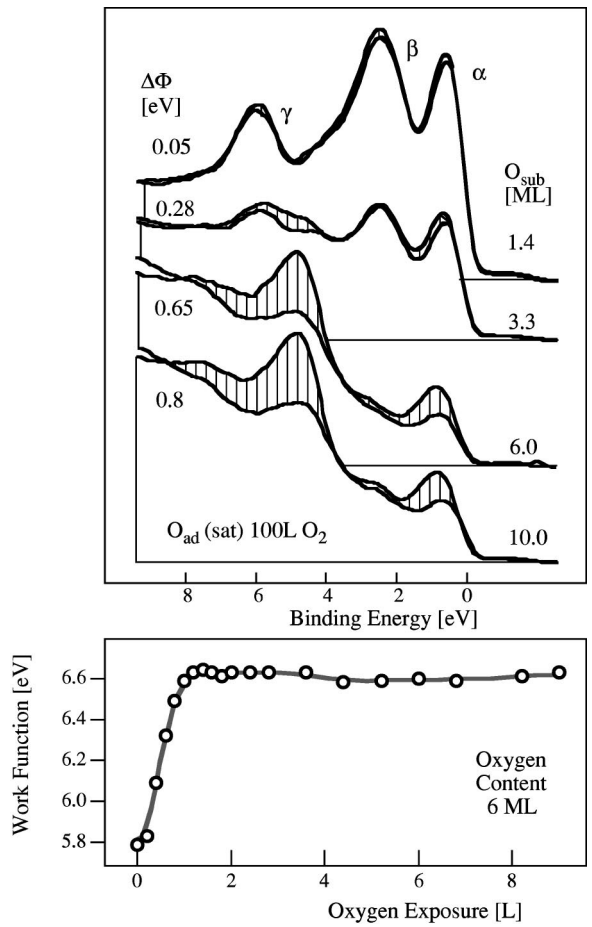

FIG. 7. The upper panel shows the valence UP spectra taken before and after the deposition of 100 L of oxygen at 300 K onto four samples differing by the oxygen content in the sample. The occupation of state *C* significantly reduces the Ru-4*d* derived states. The striped areas indicate the main spectral differences. An example of the work-function evolution as monitored during oxygen adsorption onto a surface containing approximately 6 ML of oxygen in the volume, is shown in the lower panel.

Because of the low cross section for the photoionization of *s* states the emission from the 5s orbitals is entirely buried and dominated by feature α.[26] Initial oxygen chemisorption drastically reduces the intrinsic surface resonance what is reflected by a substantial weakening of peak α. The formation of an adsorbed phase is also accompanied by a pronounced increase of the work function (Fig. 6, lower panel). The completion of the adsorbed monolayer manifests itself by a maximum work function, which is by about 1.3 eV higher when compared with a clean Ru(0001) (5.3–5.4 eV). The α and γ peaks become weaker but their energy positions remain without a significant shift. In contrast, peak β shifts by 0.4 eV towards the lower binding energy, but its intensity remains only slightly influenced by the oxygen adsorption. The formation of subsurface oxygen (content higher than 1 ML) manifests itself by much larger changes of the *d*-derived features. In the range of 1–1.6 ML, a significant enhancement of all Ru 4*d* structures is observed. Further increase of the oxygen content results in a drastic depletion of peak β. For oxygen contents higher than 6 ML this spectral feature has completely disappeared. The increasing oxygen content in the subsurface region also leads to a substantial shift of peak γ by almost 1 eV back to the initial energy position obtained for the clean ruthenium surface. Finally, the peak at binding energy of 5 eV becomes very intense and dominates the spectrum. As indicated by the UP spectra, the final oxidation stage has already been reached when the sample contained more than about 6 ML of oxygen. The formation of the subsurface-oxygen phase is accompanied by a gradual decrease of the work function (lower panel on Fig. 6). This finding also corresponds well with the thermally activated formation of the subsurface phase as observed for O/Pt(100).[30]

The peak at Fermi level remains strong even for oxygen contents in the range of 20–30 ML, where a charging of the surface due to the photoionization might be expected. This finding indicates that a ruthenium surface containing a high amount of subsurface-oxygen can not be considered as a surface of insulating oxides. Instead, it represents a coexistence of oxide domains embedded in a solution of $O^{-\delta}$ in metallic Ru lattice. The charge δ localized on oxygen ions mainly originates from the Ru-5*s* conduction electrons. The initial metallicity of the sample is maintained by *d* orbitals, which are located at Fermi level and always dominate the valence spectrum, independently of the large oxygen content.

Next, the electronic properties of the adsorbed state *C* will be investigated. Figure 7 shows UP spectra of the ruthenium surface containing 1.4, 3.3, 6.0, and 10 ML of oxygen in the

subsurface region, measured before (upper profiles) and after (lower lines) the deposition of surplus oxygen at room temperature. The exposure of 100 L oxygen guaranties a saturated O_{ad} phase. The striped areas represent the main changes appearing due to the presence of the adsorbed state *C*. For a low-oxygen content in the subsurface region only a slightly reduced intensity of the three *d* spectral features can be observed. Similarly, the corresponding work function changes are negligibly low, below the energy resolution of our spectrometer. For larger subsurface-oxygen contents (>3.3 ML) the changes induced by the O_{ad} phase become more pronounced. The work function also increases continuously with the progressing oxygen content and it reaches a value of 6.3 eV on a surface accommodating 10 ML of oxygen. The α and γ states are strongly depleted by an increasing population of the adsorbed state. In contrast, these peaks were not much affected by the preceding formation of the subsurface-oxygen phase. This difference indicates that α and γ originate from Ru orbitals, which directly participate in the binding with O_{ad}.

The lower panel in Fig. 7 shows how the oxygen adsorption on a surface containing 6 ML of oxygen influences the work function. The work function increases with the progressing occupation of the state and it saturates very soon, i.e., far before the saturation coverage, $\Theta_{ad,sat}$ is reached. The work function at saturation is by 1.3 eV higher compared with the clean Ru surface. As shown in Fig. 6 the formation of a subsurface phase is accompanied by a gradual decrease of the work function towards the value of a clean Ru surface. In contrast, the increasing population of the state raises the work function up to 6.6 eV. This evolution reflects the process of oxygen adsorption on an oxide phase terminated among others also by Ru-*d* orbitals. The large work-function increase becomes plausible when considering that the negatively charged oxygen adatoms can easily be polarized in the image potential of the substrate.[21] Since the ruthenium substrate does not lose its metallic nature due to the progressing oxidation, the substrate electrons can be transferred into the O-2*p* state. Consequently, an image-potential mediated interaction might also effectively contribute to the adsorptive bond.[27–29]

It should be added that the electronic changes described above are entirely reversible, i.e., both, the work function as well as the whole UP spectra of an initial state can be completely reproduced by heating the sample up to 600 K and desorbing the O_{ad} phase. Subsequent exposure of the sample to oxygen also results in the same O_2-TD profile, i.e., the total number of adsorption sites is not reduced by the applied heating procedure (up to 600 K).

C. Reactivity of the adsorbed state

A common way to characterize a new phase is to determine its reactivity. We have chosen the CO/CO_2 conversion process as a well-understood model reaction taking place at surfaces terminated by atomic oxygen. We conducted the following experiments: state *C* has been prepared as described above, and kept at a constant temperature of 350 K during the scattering of CO molecules. The resulting CO_2 flux was monitored by a quadruple mass spectrometer, which was placed in a specular direction with respect to the impinging CO beam. All experiments were performed using a continuous CO primary flux of 3×10^{14} molecule/cm^{2}s at which only a negligibly small increase of the background CO_2 emission in a range of 1% could be observed. Figure 8 shows the kinetics of the CO_2 production as a function of the O_{ad} coverage. The results have been obtained for a sample containing about 10 ML of subsurface oxygen. It becomes evident that the presence of adsorbed oxygen atoms substantially modifies the kinetics of the CO_2 formation: The active production stage becomes longer with increasing O_{ad} coverage. For $\Theta_{ad}=0$, i.e., with an unoccupied state *C*, the CO_2 emission appears without any delay with a very high efficiency, and becomes negligibly low within the next 3–4 s. This very early reaction component could originate from the CO interaction with some oxygen atoms belonging to the 1×1-O phase as well as to the present oxide domains. However, the early reaction component becomes substantially reduced when the oxide domains are partly covered by O_{ad}, i.e., the new oxygen atoms hinder the access of the CO molecules to the adsorption sites offered by state *C* as well as to the borders of the surrounding 1×1-O regions. This implies that not the whole 1×1-O phase but its borders participate in the early reaction component. The intensity of the early CO_2 emission becomes linearly reduced with increasing O_{ad} coverage. The early component is followed by a second maximum intensity appearing within a much longer time period which depends simply on the lateral density of the O_{ad} atoms. Thus, this clearly distinguishable, late reaction component originates from the interaction of O_{ad} atoms and CO molecules coadsorbed within the oxide domains. The reaction kinetics strongly depends on the sample temperature during the exposure to CO what suggests that the lateral mobility of the two reactants represents the limiting factor. A

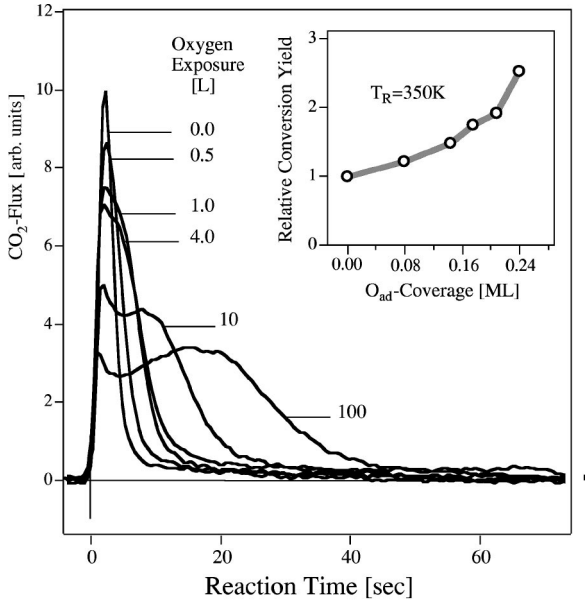

FIG. 8. The kinetics of the CO_2 emission monitored during the scattering of a CO beam on a sample containing 10 ML of oxygen in the volume and different amounts of oxygen atoms adsorbed in state *C*. The reaction was performed at surface temperature of 350 K. The inset shows the total yield of the CO oxidation normalized for a reaction conducted over a sample with an empty state *C*, $\Theta_{ad}=0$.

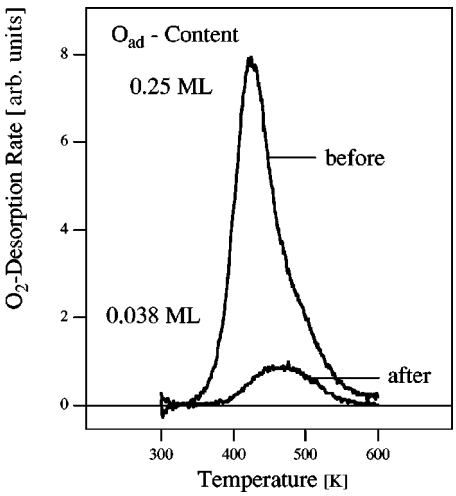

FIG. 9. O_2 TD spectra show the depletion of state *C* induced by exposing an oxygen-rich sample to 5 L of CO at 350 K. The sample contained 0.25 ML of oxygen in state *C* and about 10 ML of bulk oxygen.

more detailed model of the reaction kinetics will be published after completing our molecular beam experiments supported by isotopes exchange.

The inset in Fig. 8 shows the resulting relative reaction yield (area under the kinetics profiles normalized to the case of $\Theta_{ad}=0$) versus the progressing coverage of the adsorbed phase. As can be seen, the surplus oxygen atoms substantially enhance the integral reactivity of the surface oxygen. At maximum coverage ($\Theta_{ad}=0.24$) the total reaction yield is almost three times larger than in the case without surplus oxygen atoms. Reminding that the total number of oxygen atoms occupying state *C* is only a quarter of a monolayer, the high reactivity of the O_{ad} phase becomes evident.

In order to compare the reactivity of the selected adsorbed oxygen atoms with other known oxygen species, we conducted the final experiment which allows to estimate the integral CO/CO_2-conversion probability. For this aim, 10 ML of oxygen have been accommodated at the subsurface region and subsequently a saturated adsorbed phase has been created by an additional oxygen deposition (40 L at 300 K). Such a surface has been exposed to 5 L of CO at 350 K and the remaining oxygen population in the adsorbed state has been measured by taking an O_2-TD spectrum in the range of 300–600 K. Figure 9 shows the occupation of state *C* before and after performing the exposure to CO. The resulting conversion probability reaches a value of 0.18, which is the highest found for this reaction. It is one order of magnitude higher than the reactivity measured over a hot surface containing a rich subsurface-oxygen phase.[13] This finding suggests that the CO oxidation performed at room temperature should be substantially enhanced by applying properly chosen CO and O_2 partial pressures. Unfortunately, the rather low population of the adsorbed state in respect to the rich subsurface phase will probably reduce the total yield. Nevertheless, this chance also seems to be very attractive for other surface reactions of relevance for industrial applications. In particular, for all reactions of organic molecules proceeding via nucleophilic addition of atomic oxygen as well as for Brønsted reactions between proton transferring C-H bonds and atomic-oxygen acceptors.[1]

IV. SUMMARY

In conclusion, we have used TDS, UPS, and reactive molecular beam scattering in order to identify and characterize a oxygen-adsorbed state. The main properties of this oxygen phase are listed below.

This state can be formed at room temperature only after a rich subsurface-oxygen phase was created (oxygen content >2 ML). It reaches a saturation already at oxygen exposures lower than about 10 L. This is due to a rather high initial probability for the accommodation of an oxygen atom in this state ($S=0.7$) as well as due to a rather low capacity of this state, which has been found to depend on the oxygen content in the crystal. In all cases it is lower than 0.25 ML.

Atomic oxygen is probably bound to some sites offered by oxide domains in the topmost layer of the surface. The activation energy for associative molecular desorption depends on the oxygen content in the bulk, it ranges from 0.75 to 0.63 eV. Two Ru-4*d* bands associated with peaks α and γ were found to be involved in the bond formation. Increasing population of state *C* drastically raises the work function by 1.3 eV, which can only be explained by a strong polarization of O_{ad} atoms. Thus, either a substantial electron charge redistribution has been induced by the bonding of O_{ad} to the Ru_xO_y domains, or a pronounced charging of the O-2*p* derived state exists. The later cannot be excluded despite the fact that no direct evidence for an occupation of this state could be found by the means of UPS.

The adsorbed oxygen strongly participates in the CO/CO_2 conversion, i.e., the presence of this phase significantly modifies the kinetics and raises the integral conversion yield by more than one order of magnitude. The high oxidation probability found here (0.18) implies an appreciable relevance of this state for catalytic reactions as performed under high pressure conditions. In particular, the adsorbed oxygen phase offers a chance to reach a high reaction yield at a much lower sample temperature than the one recently found to be optimum.[13]

ACKNOWLEDGMENTS

Financial support of the Deutsche Forschungsgemeinschaft (DFG-Ni452) is gratefully acknowledged. The authors are grateful for stimulating discussions with G. Ertl, J. Behm, and K. Christmann.

*Author to whom correspondence should be addressed. Present address: Fritz-Haber-Institut der Max-Planck-Gesellschaft, Faradyweg 4-6, 14195 Berlin, Germany. FAX: +49 (0)30 84135 603. Electronic address: boettcher@fhi-berlin.mpg.de

[1] R. J. Madix and J. T. Roberts, in *Surface Reactions*, edited by R. J. Madix, Springer Series in Surface Sciences Vol. 34 (Springer-Verlag, Berlin, 1994), pp. 5–50.

[2] T.E. Madey, H.A. Engelhardt, and D. Menzel, Surf. Sci. **48**, 304 (1975).

[3] I. Surnev, G. Rangelov, and G. Bliznakov, Surf. Sci. **159**, 299 (1985).

[4] C. Stampfl, S. Schwegmann, H. Over, M. Scheffler, and G. Ertl,

Phys. Rev. Lett. **77**, 3371 (1996).
[5] C. Stampfl and M. Scheffler, Phys. Rev. B **54**, 2868 (1996).
[6] P. He and K. Jacobi, Phys. Rev. B **55**, 4751 (1997).
[7] C. Stampfl and M. Scheffler, Surf. Sci. **377-379**, 808 (1997).
[8] A. Böttcher and H. Niehus, J. Chem. Phys. **110**, 3186 (1999).
[9] W.J. Mitchell and W.H. Weinberg, J. Chem. Phys. **104**, 9127 (1996).
[10] B.A. Banse and B.E. Koel, Surf. Sci. **232**, 275 (1990).
[11] I.J. Malik and J. Hrbek, J. Vac. Sci. Technol. A **10**, 2565 (1992).
[12] J. Hrbek, D.G. van Campen, and I.J. Malik, J. Vac. Sci. Technol. A **13**, 1409 (1995).
[13] A. Böttcher, H. Niehus, S. Schwegmann, H. Over, and G. Ertl, J. Phys. Chem. B **101**, 11 185 (1997).
[14] Lj. Atanasoska, W.E. O'Grady, R.T. Atanasoski, and F.H. Pollak, Surf. Sci. **202**, 142 (1988).
[15] B. Poelsema and G. Comsa, *Scattering of Thermal Energy Atoms from Disordered Surfaces*, Springer Tracts in Modern Physics Vol. 15 (Springer-Verlag, Berlin, 1989).
[16] A.M. de Jong and J.W. Niemantsverdriet, Surf. Sci. **233**, 355 (1990).
[17] C.M. Chan, R. Aris, and W.H. Weinberg, Appl. Surf. Sci. **1**, 360 (1978).
[18] K. Joyce, P.J. Grout, and N.H. March, Surf. Sci. **181**, 141L (1987).
[19] K. Nagai and K.H. Bennemann, Surf. Sci. **260**, 286 (1992).
[20] H.-J. Freund, H. Kuhlenbeck, M. Neumann, in *Adsorption on Ordered Surfaces of Ionic Solids and Thin Films*, Springer Series in Surface Sciences Vol. 33 (Springer-Verlag, Berlin, 1993).
[21] G. Pacchioni, G. Cogliandro, and P.S. Bagus, Int. J. Quantum Chem. **42**, 1115 (1992).
[22] M.C. Wheeler, D.C. Seets, and C.B. Mullins, J. Vac. Sci. Technol. A **14**, 1572 (1996).
[23] D.A. King and M.G. Wells, Surf. Sci. **29**, 454 (1972).
[24] C. Park, Surf. Sci. **203**, 395 (1988).
[25] P. Hofmann and D. Menzel, Surf. Sci. **152/153**, 382 (1985).
[26] J. J. Yeh, *Atomic Calculations of Photoionization Cross-sections and Asymmetry Parameters* (Gordon and Breach, Langhorne, 1993).
[27] L. Surnev, G. Rangelov, and M. Kiskinova, Surf. Sci. **179**, 283 (1987).
[28] V. E. Henrich and P. A. Cox, *The Surface Science of Metal Oxides* (Cambridge University Press, Cambridge, 1993).
[29] P. Jennings, R. Jones, and M. Weinert, Phys. Rev. B **37**, 6113 (1988).
[30] J. Lauterbach, K. Asakura, and H. H. Rotermund, Surf. Sci. **313**, 52 (1999).